RSC Chemical Biology

ROYAL SOCIETY OF CHEMISTRY

PAPER

View Article Online
View Journal | View Issue

Cite this: *RSC Chem. Biol.*, 2022, 3, 1422

Chemical synthesis of the EPF-family of plant cysteine-rich proteins and late-stage dye attachment by chemoselective amide-forming ligations†

Nandarapu Kumarswamyreddy, ‡[ab] Ayami Nakagawa, ‡[a] Hitoshi Endo,[a] Akie Shimotohno,[a] Keiko U. Torii, [ac] Jeffrey W. Bode [ad] and Shunsuke Oishi *[a]

Received 23rd June 2022,
Accepted 18th October 2022

DOI: 10.1039/d2cb00155a

rsc.li/rsc-chembio

Chemical protein synthesis can provide well-defined modified proteins. Herein, we report the chemical synthesis of plant-derived cysteine-rich secretory proteins and late-stage derivatization of the synthetic proteins. The syntheses were achieved with distinct chemoselective amide bond forming reactions – EPF2 by native chemical ligation (NCL), epidermal patterning factor (EPF) 1 by the α-ketoacid-hydroxylamine (KAHA) ligation, and fluorescent functionalization of their folded variants by potassium acyltrifluoroborate (KAT) ligation. The chemically synthesized EPFs exhibit bioactivity on stomatal development in *Arabidopsis thaliana*. Comprehensive synthesis of EPF derivatives allowed us to identify suitable fluorescent variants for bioimaging of the subcellular localization of EPFs.

Introduction

Chemically functionalized proteins are important research tools for elucidating and visualizing biological pathways. Reporter groups, such as fluorescent dyes[1,2] and radioactive groups,[3,4] introduced onto protein probes enable the monitoring of their dynamics in complex biological systems. A number of labeling methods were developed to introduce functionalities onto natural residues of proteins,[5–8] including attachments to lysine,[9–11] cysteine,[12–15] tyrosine,[16] tryptophan,[17] methionine,[18] N- or C-termini.[19] However, these techniques usually result in a heterogeneous mixture of functionalized proteins as most proteins contain multiple reactive natural residues.

Chemical synthesis of proteins, accomplished by chemoselective amide bond forming reactions *i.e.* peptide ligations, provides an alternative approach to structurally uniform protein probes.[20–26] Precisely controlled structure of chemically synthesized protein probes could exclude artefacts caused by a heterogeneous or structurally-deficient protein probes.[27–29] Despite the advantage of chemically synthesized protein probes, synthesis is often a tedious and time-consuming process, especially if key reporter groups are introduced at the early stage of synthesis by incorporating modified amino acid monomers at the peptide elongation process. After construction of the peptide chain, peptides are cleaved from the resin, purified by HPLC, ligated to yield proteins, and finally refolded into the biologically active form. Optimization of the reporter groups often requires that nearly the entire synthesis needs to be repeated to give variants of the probe. As the result, optimization of the probe structure for each biological experiment often becomes a bottleneck.

In order to easily decorate folded proteins, we have developed the KAT ligation, a rapid chemoselective amide bond-forming reaction between potassium acyltrifluoroborates (KATs) and *O*-carbamoylhydroxylamines.[4,30–34] KAT ligation has been applied in site-specific functionalization, such as PEGylation, lipidation, biotinylation, and dye labeling of chemically synthesized peptides and proteins bearing hydroxylamine at low concentrations in aqueous buffers with near equimolar amounts of the ligation partners.[30,32,35–37] Functionalization of chemically synthesized proteins bearing hydroxylamine using KATs would allow us to access protein probes bearing various reporter groups and select quickly suitable protein probes for chemical biology studies.

We chose the EPF-family of secretory cysteine-rich proteins (CRPs) for our study.[38–40] CRPs are a ubiquitous family of

[a] *Institute of Transformative Bio-Molecules (WPI-ITbM), Nagoya University, Chikusa Nagoya 464-8602, Japan. E-mail: oishi@itbm.nagoya-u.ac.jp*
[b] *Department of Chemistry, Indian Institute of Technology Tirupati, Tirupati, 517619, Andhra Pradesh, India*
[c] *Howard Hughes Medical Institute and Department of Molecular Biosciences, The University of Texas at Austin, Austin, TX 78712, USA*
[d] *Department of Chemistry and Applied Biosciences, ETH Zürich, Zürich 8093, Switzerland*

† Electronic supplementary information (ESI) available. See DOI: https://doi.org/10.1039/d2cb00155a

‡ These authors contributed equally.

Fig. 1 Amino acid sequences of EPFL9, EPF2, and EPF1.

proteins found in all kingdoms of life and often play crucial roles in intercellular signaling.[41–47] Particularly in plants, CRPs participate in reproductive processes,[48–50] tissue and seed development,[51–54] and plant immune systems.[55–57] Among the eleven EPF members, at least three of them, EPFL9 (also known as STOMAGEN), EPF2, and EPF1 play a key role in regulating formation of stomata, which control gas exchange by opening and closing of pores on the plant surface.[39,40,58–62]

EPFL9, EPF2, and EPF1 contain 45–52 amino acid residues with six or eight cysteine residues within the protein sequence (Fig. 1).[63] These cysteine residues require disulfide bond formation to impart biological functions into the proteins, and on the other hand cysteine residues cause low-yielding of recombinant expression of EPFs in *E. coli* due to premature disulfide formations and protein aggregation.[64,65] High purity of synthetic precursors of oxidative folding is advantageous to obtain folded active EPFs. Furthermore, late-stage chemical functionalization of folded EPFs will enable us to develop structurally well-defined protein probes and choose a suitable functionalization for chemical biology studies of EPF proteins.

In this report, we document the chemical synthesis of EPF-family plant CRPs and late-stage functionalization by chemoselective amide bond forming reactions. EPFL9 was synthesized by solid-phase peptide synthesis (SPPS), EPF2 through native chemical ligation (NCL), and EPF1 *via* chemoselective α-ketoacid-hydroxylamine (KAHA) ligation. After folding, the synthetic CRPs were functionalized with various fluorescent dyes by chemoselective KAT ligation onto a hydroxylamine moiety installed at the N-terminus. This late-stage functionalization strategy allowed us to produce and evaluate a varieties of protein probes. The chemically synthesized EPFL9, EPF2, EPF1, and their variants exhibited biological activity in *Arabidopsis* plants.

Results and discussion

Synthesis of EPFs by Fmoc SPPS

The reduced EPFL9 **1a** was successfully synthesized by standard Fmoc SPPS and isolated in 42% yield after RP-HPLC purification (Fig. 2). However, the coupling efficiency of Cys27, Ser28, and Val29 in EPF2, and Phe25, Val26, and Cys27 in EPF1 were very low and the target peptides were not observed after these residues. Therefore, we elected to employ peptide ligation strategy by assembling peptide segments of EPF2 and EPF1 proteins into full length proteins.

Synthesis of EPF2 protein by NCL

We carefully examined the amino acid sequence of EPF2 and designed a ligation site between Ser32–Cys33 for NCL

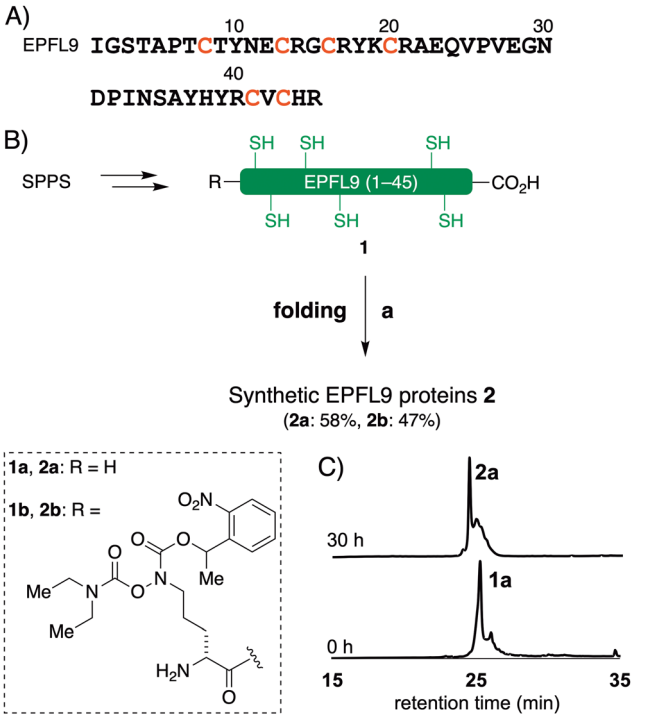

Fig. 2 Chemical synthesis of EPFL9. (A) Amino acid sequence of EPFL9. (B) Chemical synthesis of EPFL9. Reagents and conditions: (a) 6 M Gdn·HCl, 0.1 M tris pH 6.8 then add 0.1 M tris 5.0 mM reduced glutathione 2.5 mM oxidized glutathione pH 8.0, 4 °C, 30 h. (C) Analytical HPLC traces (λ = 220 nm) of monitoring of folding of **1a**.

(Fig. 3).[21–25] The peptide thioester segment **3a** can be prepared from a peptide hydrazide precursor, which can be synthesized by standard Fmoc SPPS.[66] Methionine residues Met22 was substituted with norleucine (Nle) and all cysteine residues were protected with Acm protecting groups.

The peptide thioester segment **3a** was obtained *via* Fmoc SPPS on 0.47 mmol scale using 2-Cl-(Trt)-$NHNH_2$ resin followed by oxidation and addition of β-mercaptopropionic acid[66] (see ESI,† Section S3.1). The peptide segment **4** containing a cysteine residue at the N-terminus was synthesized on a 0.32 mmol scale by standard Fmoc SPPS. After trifluoroacetic acid (TFA) cleavage from the resin, the resulting peptide was purified and obtained 260 mg of segment **4** in 32% yield.

With segments **3a** and **4** in hand, we examined NCL between peptide thioester segment **3a** (1.0 equiv.) and peptide segment **4** (1.1 equiv.) with optimized reaction conditions (6 M Gdn·HCl, 0.2 M Na_2HPO_4, 100 mM TCEP, 100 mM sodium ascorbate, 3% (v/v) thiophenol, pH 7.4) gave the ligated peptide **5a** in 67% yield (Fig. 3B). The cysteine Acm group of **5a** was deproptected and **6a** was purified by preparative RP-HPLC and isolated in 70% yield.

Synthesis of EPF1 protein by KAHA ligation

The KAHA ligation[67–75] operates under acidic conditions with water/organic solvent mixture ideal for solubilizing hydrophobic segments and resulting in more soluble peptide esters such as *O*-acyl isopeptide or depsi peptide as a primary ligation

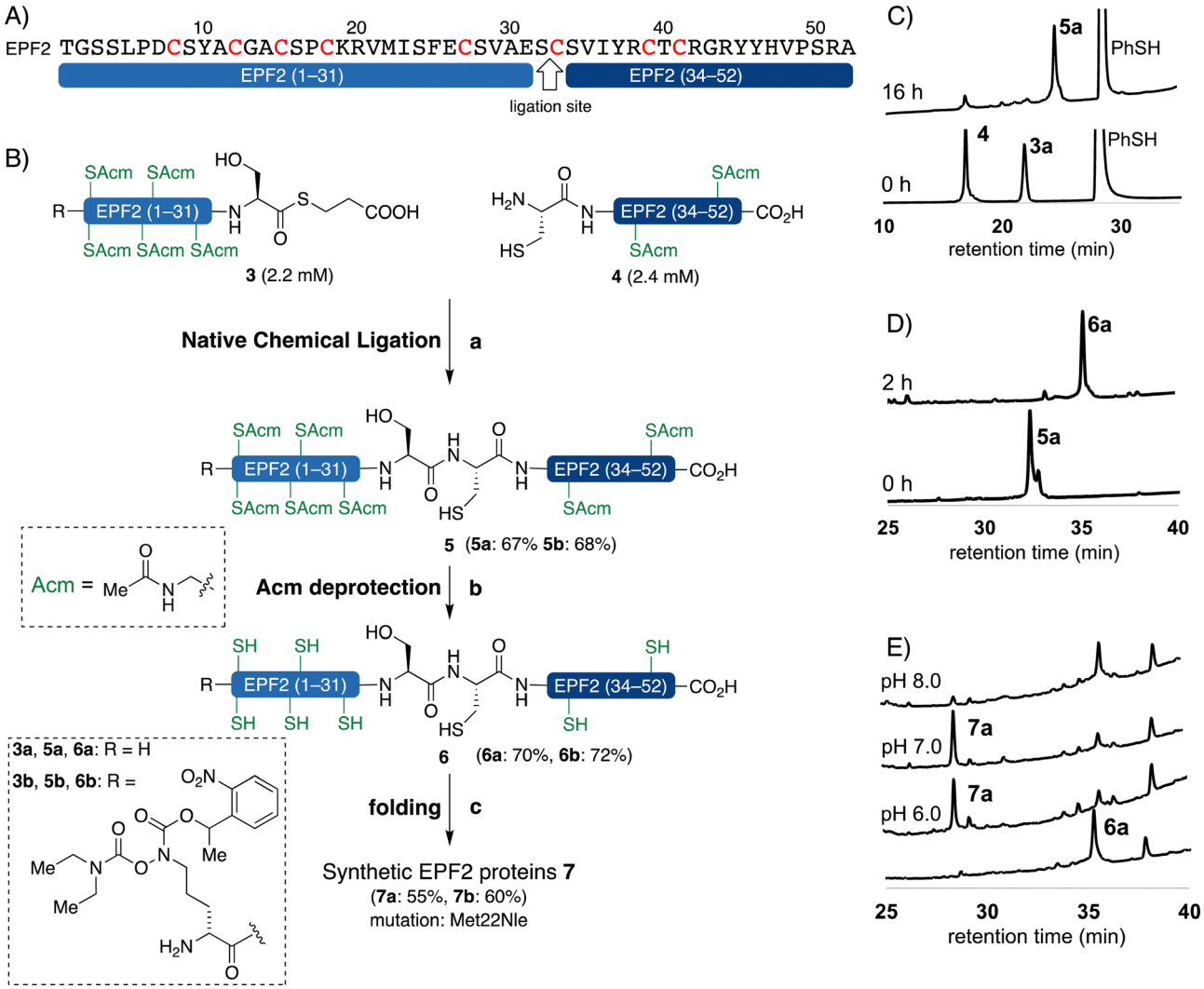

Fig. 3 Chemical synthesis of EPF2 by NCL. (A) Amino acid sequence of EPF2 showing the ligation site. (B) Chemical synthesis of EPF2 by NCL, reagents and conditions: (a) 3% (v/v) PhSH, 6 M Gdn·HCl, 0.2 M Na_2HPO_4, 100 mM TCEP, 100 mM sodium ascorbate, pH = 7.4, rt, 16 h, **5a**: 67% **5b**: 68%; (b) 1% AgOAc in 1 : 1 AcOH/H_2O (w/v/v), 45 °C, 2 h; (c) 6 M Gdn·HCl, 0.1 M tris buffer pH 6.8, then add 0.1 M tris, 5.0 mM reduced glutathione 2.5 mM oxidized glutathione, pH 7.0, 4 °C, 30 h. (C) Analytical HPLC traces (λ = 220 nm) of monitoring the ligation between **3a** and **4**. (D) Analytical HPLC traces (λ = 220 nm) of monitoring the Acm deprotection of **5a**. (E) Analytical HPLC traces (λ = 220 nm) of folding of **6a**.

product. After rearrangement of the ligated product under the basic conditions, the resulting polypeptide contains a non-canonical amino acid residue homoserine (Hse), when using 5-oxaproline as a ligation handle on the N-terminus of the C-terminal peptide fragment.[67,71]

We designed the KAHA ligation site between Val30–Glu31 as SPPS was successful up to Ala28 from the C-terminus (Fig. 4). The preparation of peptides bearing C-terminal valine α-ketoacids is well established. The ligation site at this particular position introduces a Hse residue as a Glu31Hse mutation. The three methionine residues Met28, Met38, Met43 were substituted with Nle to avoid oxidation during handling, storage and folding (Fig. 4B). We expected that these changes in the protein sequence would be unlikely to have a strong effect on protein structure and biological activity. We selected acetamidomethyl (Acm) protecting group for all cysteine residues to avoid premature formation of intra- and intermolecular disulfide bond formation during HPLC purification and ligation of the peptide segments.

We performed the synthesis of peptide segment EPF1 (1–30) with an α-ketoacid using standard Fmoc-protected amino acids and protected valine α-ketoacid resin with 0.25 mmol g^{-1}. After TFA cleavage from the resin, the resulting peptide was difficult to analyze and purify with RP-HPLC due to poor solubility to aqueous acetonitrile with 0.1% TFA. To overcome the solubility issue, we incorporated two Gly–Ser *O*-isoacyl dipeptide units into the peptide segment. This strategy was developed by Mutter and Kiso groups, and known to enhance the solubility of the resulting synthetic peptide.[76–79] This Gly–Ser *O*-isoacyl dipeptide strategy fits well with the KAHA ligation, as the esters can be rearranged into peptide bonds under basic conditions together with depsipeptide bond resulted by the KAHA

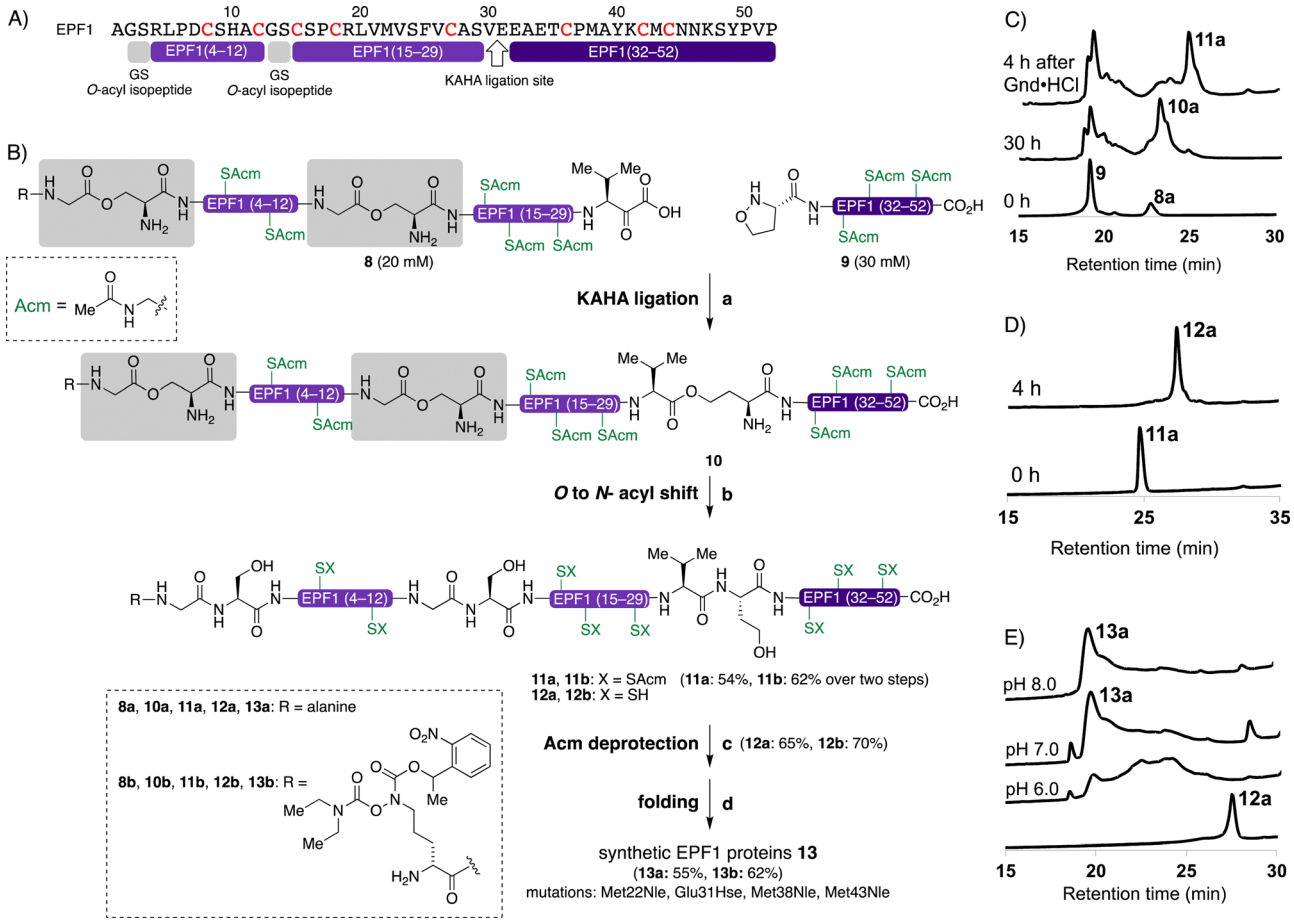

Fig. 4 Chemical synthesis of EPF1 by KAHA ligation. (A) Amino acid sequence of EPF1 showing the ligation site and Gly–Ser *O*-acylisopeptides. (B) Chemical synthesis of EPF1 by KAHA ligation, reagents and conditions: (a) 0.1 M oxalic acid 9 : 1 DMSO/H_2O (v/v), 60 °C, 30 h; (b) 6 M Gdn·HCl, pH 9.6, 4 h, rt; (c) 1% AgOAc in 1 : 1 AcOH/H_2O (w/v/v), 45 °C, 2 h: (d) 6 M Gdn·HCl, 0.1 M tris buffer pH 6.8 then add 0.1 M tris, 5.0 mM reduced glutathione, 2.5 mM oxidized glutathione, pH 8.0, 4 °C, 30 h. (C) Analytical HPLC traces (λ = 220 nm) of monitoring the ligation between **8a** and **9**, and *O* to *N*-acyl shift. (D) Analytical HPLC traces (λ = 220 nm) of monitoring the Acm deprotection of **11a**. (E) Analytical HPLC traces (λ = 220 nm) of folding of **12a**.

ligation.[80] We resynthesized segment **8a** with two N_α-boc protected Gly–Ser *O*-isoacyl dipeptides at position 2–3 and 13–14 during Fmoc-SPPS with 0.25 mmol g^{-1} on protected valine α-ketoacid resin. We were pleased to observe good solubility of peptide segment **8a** containing two *O*-isoacyl dipeptides in aqueous acetonitrile, and the crude peptide segment was purified by RP-HPLC; and 102 mg of pure segment **8a** were isolated in 12% yield (see ESI,† Section S4.1).

We synthesized the peptide segment **9** containing an N-terminal 5-oxaproline by Fmoc-SPPS on resin with 0.3 mmol $gram^{-1}$ followed by TFA cleavage from resin. After purification by preparative RP-HPLC we obtained 160 mg of purified peptide segment **9** in 20% yield (see ESI,† Section 4.3).

With pure segments **8a** and **9** in hand, we performed KAHA ligation between α-ketoacid segment **8a** (1.0 equiv., 20 mM), with 5-oxaproline segment **9** (1.5 equiv., 30 mM) in 9 : 1 (v/v) DMSO/water. The acidic reaction conditions of KAHA ligation and Gly–Ser *O*-isoacyl moieties were beneficial for solubilizing **8a**. The ligation product **10a**, containing three ester bonds was formed in 30 h (Fig. 4B). We performed *in situ O* to *N*-acyl shift by diluting the ligation mixture with 10-fold volume of 6 M guanidine hydrochloride (Gdn·HCl), adjusting the pH to 9.6, and stirring at room temperature for another 4 h. A significant retention time shift was observed in analytical RP-HPLC and the rearranged peptide **11a** was purified by preparative RP-HPLC and 26 mg of **11a** obtained in 54% overall yield after two steps. Hydrolyzed products of the ester bonds were not observed.

The cysteine Acm deprotection of **11a** was performed by dissolving peptide in 1% AgOAc in 50% aqueous AcOH at 45 °C for 2 h. The resulting reduced peptide **12a** was purified RP-HPLC and isolated in 65% yield.

Oxidative folding of EPFs

With the reduced EPFs **1a**, **6a**, and **12a** in hand, we optimized the folding conditions in two sequential steps. First, the reduced EPFs were dissolved (0.5 mM concentration) in denaturing buffer (6 M Gdn·HCl, 0.1 M tris(hydroxymethyl)amine hydrochloride (Tris·HCl) pH 6.8) at room temperature open to air. After 1 h, the denatured EPFs were diluted 8-fold with folding buffer (60 μM, final concentration). Different pH values of folding buffer and additives were tested. The best results were obtained by using the following refolding buffer: 1 M Gdn·

HCl, 5.0 mM reduced glutathione, and 2.5 mM oxidized glutathione, pH 8.0 for EPFL9; pH 7.0 for EPF2; pH 8.0 for EPF1, at 4 °C for 30 h on a shaker. After purification using preparative RP-HPLC we isolated folded EPFL9 protein **2a** (58% isolated yield), EPF2 protein **7a** (55% isolated yield), and EPF1 protein **13a** (55% isolated yield). The identity was confirmed by ESI-HRMS analysis.

Bioactivity of synthetic EPFs

We evaluated the bioactivity of our chemically synthesized EPFs on Arabidopsis wild type plants. It is known that EPFL9 stimulates stomatal development, while EPF2 and EPF1 inhibit it.[58–61] As shown in Fig. 5, the stomatal density of cotyledons treated with reduced EPFL9 **1a** and folded EPFL9 **2a** were 1.4-fold and 2.1-fold higher than those for mock, respectively.

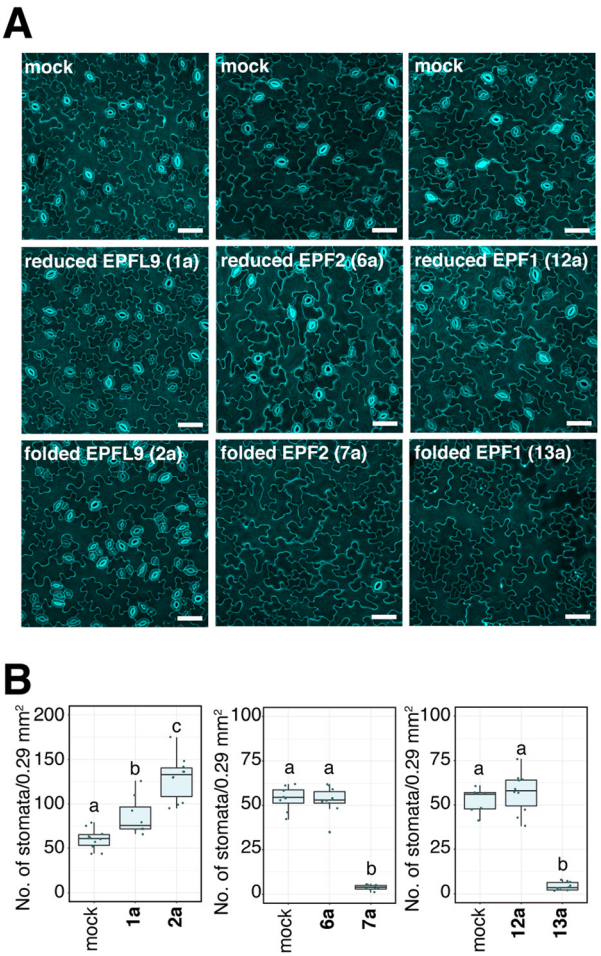

Fig. 5 Bioactivity of synthetic EPFs on stomatal formation: (A) representative confocal images of cotyledon abaxial epidermis from the 7-day-old Arabidopsis wild type Col-0 seedlings treated with mock (top), reduced EPFs (middle) or folded EPFs (bottom). Scale bar = 50 μm. (B) Quantitative analysis of the number of stomata shown as a box plot. Dots, individual data points. Median values are shown as lines in the boxplot. ANOVA after Tukey's HSD test was performed for comparison of samples treated with the mock and each peptide. Number of leaves analyzed, n = 8, 10, 10, 8, 10, 9, 10, 8, 10 for treatment with mock (for EPFL9), reduced EPFL9 **1a**, folded EPFL9 **2a**, mock (for EPF2), reduced EPF2 **6a**, folded EPF2 **7a**, mock (for EPF1), reduced EPF1 **12a**, folded EPF1 **13a**, respectively. Letters indicate significant difference ($P < 0.05$).

When treated with synthetic folded EPF2 **7a** and folded EPF1 **13a**, the numbers of stomata in leaves were significantly reduced (7.2% and 8.1% compared with each mock treatment). In contrast, reduced EPF2 **6a** or EPF1 **12a** did not affect stomatal numbers (Fig. 5). These results indicate that synthetic EPFs have activity on stomatal development as the activities are comparable with previous reports.[63,81,82]

Synthesis of EPFs with a KAT ligation handle

In order to introduce reporter groups onto EPF with site-specifically and acquire suitable probes to visualize dynamics of EPF proteins *in vivo*, we incorporated a hydroxylamine at N-terminus of EPFs, which allows introduction of fluorescent dyes with site selective manner to folded proteins.

The reduced EPFL9 **1b** was synthesized by standard Fmoc SPPS and introduction of ornithine hydroxylamine with photo labile protecting group (Orn HA) HA at N-terminus. We resynthesized the segments **3** and **8** with KAT ligation handle by introducing Orn HA, which we reported previously[31] at the N-terminus during Fmoc SPPS. The thioester segment **3b** and α-ketoacid segment **8b** were obtained in 46% and 16% yield, respectively. NCL of thioester segment **3b** and **4** gave Acm protected ligation product **5b** in 68% yield. The KAHA ligation reaction was performed between **8b** and **9** using previously established EPF1 ligation conditions, followed by *O* to *N*-acyl shift. The Acm protected EPF1 **11b** was isolated in 62% yield (over two steps). The reduced EPF2 **6b** and EPF1 **12b** were obtained in 72% and 70% yield, respectively. The reduced proteins **1b**, **6b** and **12b** were folded using previously optimized folding conditions.

Fluorescent labelling of EPF proteins by KAT ligation

We envisioned visualizing the subcellular localization of EPFs by fluorescent labeling of EPFs and fluorescent microscopy.[83–85] In

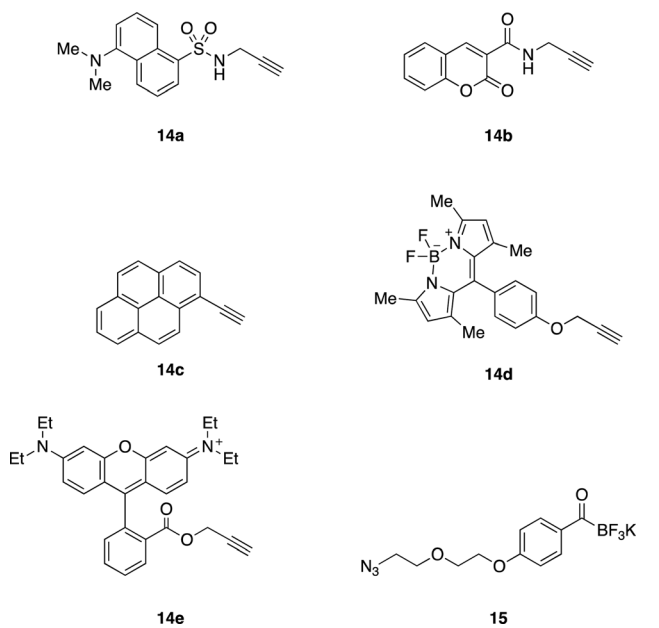

Fig. 6 Alkyne containing dyes **14a–e** and azido functionalized KAT **15**.

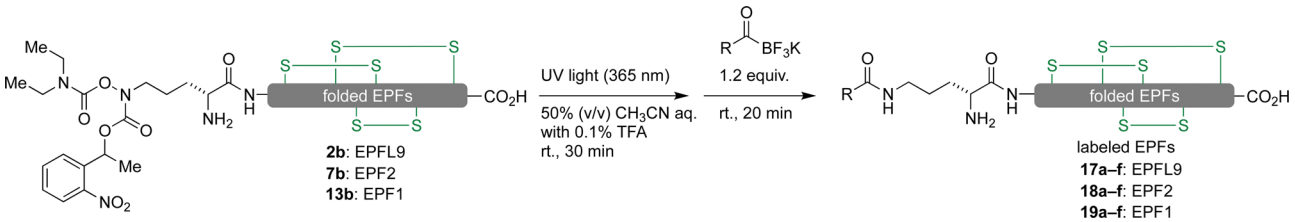

	folded EPFs	labeled EPFs (isolated yield)
16a	**2b**	**17a** (52%)
	7b	**18a** (50%)
	13b	**19a** (45%)
16b	**2b**	**17b** (60%)
	7b	**18b** (72%)
	13b	**19b** (56%)
16c	**2b**	**17c** (70%)
	7b	**18c** (60%)
	13b	**19c** (57%)
16d	**2b**	**17d** (85%)
	7b	**18d** (72%)
	13b	**19d** (65%)
16e	**2b**	**17e** (84%)
	7b	**18e** (75%)
	13b	**19e** (60%)
15	**2b**	**17f** (75%)
	7b	**18f** (67%)
	13b	**19f** (62%)

Scheme 1 Fluorescent labelling of EPFs by KAT ligation.

order to find suitable fluorescent dye, we synthesized KATs **16a–e** from alkyne containing dyes **14a–e** (Fig. 6) with azido functionalized KAT **15** through azide–alkyne cycloaddition in 55–81% yields (see ESI,† Section S6).

Initially, KAT ligation of **2b** and dansyl KAT **16a** was examined. UV light (365 nm) irradiation to a mixture of **2b** (50 μM, 1.0 equiv.) and **16a** (75 μM, 1.5 equiv.) in 50% aqueous acetonitrile mixture with 0.1% TFA only gave a trace amount of the desired product in 20 min; the majority of **16a** decomposed and became unreactive towards the hydroxylamine. To prevent decomposition of the fluorophore, we first irradiated a solution of **2b** with 365 nm UV light for 30 minutes. After the complete removal of photo-labile protecting group analyzed by analytical RP-HPLC, dansyl KAT **16a** (1.2 equiv.) was added to the reaction mixture at room temperature. We were pleased to see that the reaction proceeded cleanly without decomposition of **16a** after 20 minutes and isolated the dansyl labeled EPFL9 **17a** in 52% yield (Scheme 1). Using these conditions, we functionalized folded EPF proteins, **2b**, **7b**, **13b** to a variety of dye-labeled folded EPF proteins **17a–f**, **18a–f**, and **19a–f** in 45–85% yields using KATs **16a–e** (Scheme 1).

Bioassay data of dye-labeled EPFL9 for stomatal development in *Arabidopsis* plants

We evaluated the bioactivity of dye-labeled EPFL9 **17a–e** and azide variant **17f**. As shown in Fig. 7, **17f**, the control for dye-labeled EPFL9 (in which similar reaction procedure was

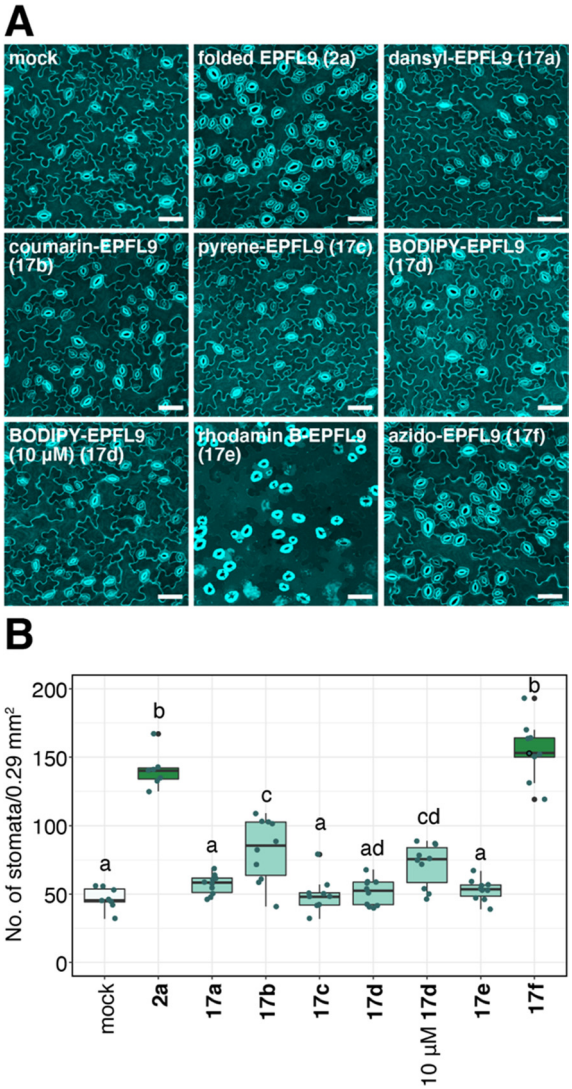

Fig. 7 Fluorescent labeled EPFL9 retain various degrees of bioactivity. (A) Representative confocal images of cotyledon abaxial epidermis from the 7-day-old Arabidopsis wild type Col-0 seedlings treated with mock, 5 μM folded EPFL9 **2a**, 5 μM azido-EPFL9 **17f** and 5 μM fluorescence-labeled EPFL9s **17a–e**. For the BODIPY-EPFL9 **17d** treatment, the image for 10 μM treatment is also shown. Scale bar = 50 μm. (B) Quantitative analysis of the number of stomata shown as a box plot. Dots, individual data points. Median values are shown as lines in the boxplot. ANOVA after Tukey's HSD test was performed for comparison of samples treated with the mock and each peptide. Number of leaves analyzed, n = 8, 7, 9, 10, 10, 10, 10, 9, 10 for treatment with mock, 5 μM folded EPFL9 **2a**, 5 μM azido-EPFL9 **17f**, 5 μM coumarin-EPFL9 **17b**, 5 μM BODIPY-EPFL9 **17d**, 10 μM BODIPY-EPFL9 **17d**, 5 μM dansyl-EPFL9 **17a**, 5 μM pyrene-EPFL9 **17c**, and 5 μM rhodamine B-EPFL9 **17e**, respectively. Letters indicate significant difference ($P < 0.05$).

conducted without adding coupling dyes) showed stomata-inducing activity as strong as non-labeled folded EPFL9 **2a.** Most EPFL9 variants (**17a–e**) except coumarin-EPFL9 **17b** showed reduced bioactivity (Fig. 7). When leaves were treated with 10 μM BODIPY-EPFL9 **17d,** the stomatal number was significantly elevated in comparison to those of the mock-treated control, indicating that BODIPY-EPFL9 **17d** retains its bioactivity (Fig. 7). Non-conjugated fluorophores alone did not impart any activity on stomatal development (ESI,† Fig. S1). It is likely that coupling of fluorescent dyes might affect EPFL9 structures, which reflect various degrees of their bioactivities.

BODIPY-EPFL9 is incorporated into *Arabidopsis* leaves

EPF peptides interact with the receptor-like kinases ERECTA-family proteins localized at the plasma membrane[81] and initiates stomatal signaling. Since BODIPY-EPFL9 **17d** retains bioactivity (Fig. 7), we sought to visualize the localization of fluorescence-labeled EPFL9 in the cotyledon epidermis. For this purpose, *Arabidopsis* seedlings were co-treated with BODIPY-EPFL9 **17d** and FM4-64 (a styryl dye that stains plasma membrane).[86] Strong BODIPY signals (yellow) were detected in the plasma membrane of stomatal precursors, co-localizing with FM4-64 signals (magenta) (Fig. 8A). Quantification of line

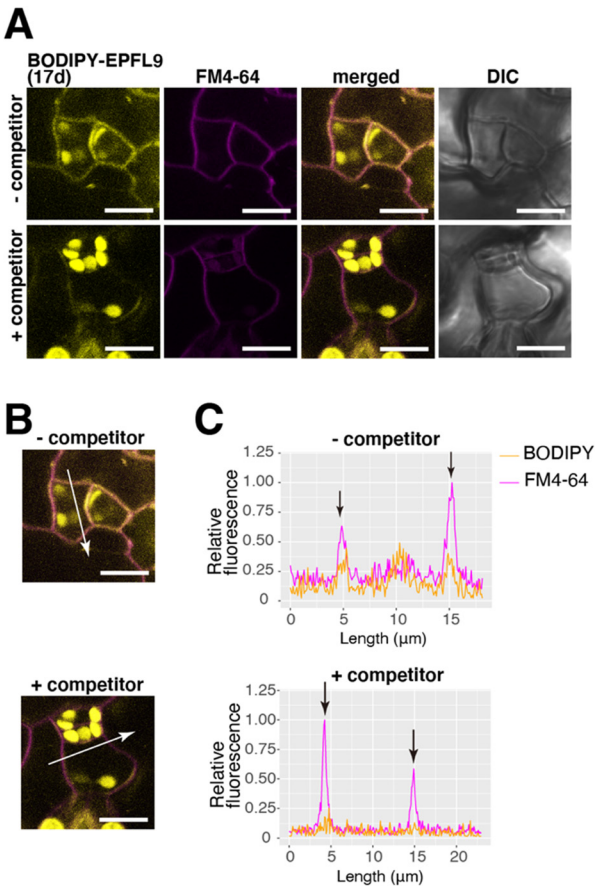

Fig. 8 BODIPY-EPFL9 **17d** is localized at the plasma membrane and competed by EPFL9 **2a**. (A) Representative confocal images of BODIPY (yellow) and FM4-64 (magenta) in the abaxial epidermis of cotyledons from the 7-day-old Arabidopsis Col-0 seedlings. The seedlings were treated with 0.6 μM FM4-64 and 6 nM BODIPY-EPFL9 **17d** with or without 6 nM non-labeled folded EPFL9 **2a** for 10 min. Scale bar = 20 μm. (B) Merged images of BODIPY and FM4-64. Scale bar = 10 μm. (C) Line plots of BODIPY (yellow) and FM4-64 (magenta) fluorescence on 1-pixel-thickness of arrow indicated in (B). Arrows indicate FM4-64 fluorescence staining the plasma membrane.

slicing showed two BODIPY/FM4-64 peaks corresponding to the plasma membrane, with signal ratio of 0.55 and 0.41, respectively (Fig. 8B and C).

In contrast, when incubating BODIPY-EPFL9 **17d** and FM4-64 in the presence of non-labeled folded EPFL9 **2a** as a competitor, no clear peaks for BODIPY signals were detected at the plasma membrane (Fig. 8A). The BODIPY/FM4-64 signal ratios at the plasma membrane were declined to 0.18 and 0.14, much lower than those incubated without non-labeled EPFL9 **2a** (Fig. 8B and C). These results indicate that BODIPY-EPFL9 **17d** was incorporated into the *Arabidopsis* epidermis. The observation that BODIPY-EPFL9 **17d** competes with the non-labeled folded EPFL9 **2a** suggests the specificity and reversible, transient nature of peptide binding. It is known that EPF2 and EPFL9 competitively bind to the receptor to fine-tune stomatal patterning,[87] and that the receptor dynamically changes its subcellular localization upon perceiving different EPF/EPFL peptides.[88] In the future, multiple visualization of ERECTA-family receptors and multiple fluorescence-labeled EPF peptides could help further understanding the behavior of their interactions.

Conclusions

In summary, EPFs were chemically synthesized by chemoselective amide bond forming reactions – EPF2 by NCL and EPF1 by KAHA ligation. Chemically synthesized EPFs showed the expected bioactivities on stomatal development in *Arabidopsis* plants. Late-stage attachment of fluorescent dyes to folded proteins were achieved by chemoselective amide bond forming reaction, KAT ligation. This efficient synthesis of the protein variants through the folded EPFs bearing hydroxylamine as a key intermediate of derivatization enabled us to identify that BODIPY-labeled EPFL9 **17d** maintains the protein activity and suitable for bioimaging study. Localization of EPFL9 to the plasma membrane was visualized by fluorescent microscopy.

The choice of fluorescent dyes is important for bioimaging studies. The late-stage functionalization strategy enabled us to prepare a variety of protein and choose a suitable variant for bioimaging.

Having now the fluorescent labeled EPF proteins, we will pursue visualization of signal perception and transduction in plants. We anticipate that this late-stage functionalization strategy of synthetic proteins should be applicable to other CRPs.

Author contributions

S. O. conceived of the idea. N. K. synthesized the EPF proteins, dye-KATs, and the labeled EPFs. A. N. and H. E. performed the stomatal development assays. A. N. and A. S. carried out the bioimaging studies. N. K., A. N., K. U. T., J. W. B. and S. O. designed the experiments and analyzed the data. K. U. T. and S. O. obtained the funding for this research project. N. K., A. N. and S. O. wrote the manuscript with help from all authors.

Conflicts of interest

The authors declare no conflict of interest.

Acknowledgements

We are grateful to Dr Keiko Kuwata (Molecular Structure Center at WPI-ITbM) for ESI-HRMS. This work was supported by JSPS KAKENHI (Grant no. 16K05842, 19K15705, 19H00990, and 22K05312). N. K., A. N., and H. E. thank to the WPI-ITbM for the fellowship. ITbM is supported by the World Premier International Research Center Initiative (WPI), Japan.

References

1 C. P. Toseland, *J. Chem. Biol.*, 2013, **6**, 85–95.
2 J. Liu and Z. Cui, *Bioconjugate Chem.*, 2020, **31**, 1587–1595.
3 A. C. Patel and S. R. Matthewson, in *Molecular Biomethods Handbook*, ed. R. Rapley and J. M. Walker, Humana Press, Totowa, NJ, 1998, p. 411.
4 A. Chiotellis, H. Ahmed, T. Betzel, M. Tanriver, C. J. White, H. Song, S. Da Ros, R. Schibli, J. W. Bode and S. M. Ametamey, *Chem. Commun.*, 2020, **56**, 723–726.
5 O. Boutureira and G. J. L. Bernardes, *Chem. Rev.*, 2015, **115**, 2174–2195.
6 N. Krall, F. P. da Cruz, O. Boutureira and G. J. L. Bernardes, *Nat. Chem.*, 2016, **8**, 103–113.
7 J. N. deGruyter, L. R. Malins and P. S. Baran, *Biochemistry*, 2017, **56**, 3863–3873.
8 S. Sakamoto and I. Hamachi, *Anal. Sci.*, 2019, **35**, 5–27.
9 K. Tanaka, K. Fukase and S. Katsumura, *Synlett*, 2011, 2115–2139.
10 P. M. S. D. Cal, J. B. Vicente, E. Pires, A. V. Coelho, L. F. Veiros, C. Cordeiro and P. M. P. Gois, *J. Am. Chem. Soc.*, 2012, **134**, 10299–10305.
11 S. Diethelm, M. A. Schafroth and E. M. Carreira, *Org. Lett.*, 2014, **16**, 3908–3911.
12 N. Lundell and T. Schreitmüller, *Anal. Biochem.*, 1999, **266**, 31–47.
13 M. D. Simon, F. Chu, L. R. Racki, C. C. de la Cruz, A. L. Burlingame, B. Panning, G. J. Narlikar and K. M. Shokat, *Cell*, 2007, **128**, 1003–1012.
14 H.-Y. Shiu, H.-C. Chong, Y.-C. Leung, T. Zou and C.-M. Che, *Chem. Commun.*, 2014, **50**, 4375–4378.
15 J. M. J. M. Ravasco, H. Faustino, A. Trindade and P. M. P. Gois, *Chemistry*, 2019, **25**, 43–59.
16 S. D. Tilley and M. B. Francis, *J. Am. Chem. Soc.*, 2006, **128**, 1080–1081.
17 W. Siti, A. K. Khan, H.-P. M. de Hoog, B. Liedberg and M. Nallani, *Org. Biomol. Chem.*, 2015, **13**, 3202–3206.
18 S. Lin, X. Yang, S. Jia, A. M. Weeks, M. Hornsby, P. S. Lee, R. V. Nichiporuk, A. T. Iavarone, J. A. Wells, F. D. Toste and C. J. Chang, *Science*, 2017, **355**, 597–602.
19 J. I. MacDonald, H. K. Munch, T. Moore and M. B. Francis, *Nat. Chem. Biol.*, 2015, **11**, 326–331.

20 T. W. Muir and S. B. Kent, *Curr. Opin. Biotechnol*, 1993, **4**, 420–427.
21 P. E. Dawson, T. W. Muir, I. Clark-Lewis and S. B. Kent, *Science*, 1994, **266**, 776–779.
22 A. C. Conibear, E. E. Watson, R. J. Payne and C. F. W. Becker, *Chem. Soc. Rev.*, 2018, **47**, 9046–9068.
23 S. B. H. Kent, *Chem. Soc. Rev.*, 2009, **38**, 338–351.
24 V. Agouridas, O. El Mahdi, V. Diemer, M. Cargoët, J.-C. M. Monbaliu and O. Melnyk, *Chem. Rev.*, 2019, **119**, 7328–7443.
25 S. S. Kulkarni, J. Sayers, B. Premdjee and R. J. Payne, *Nat. Rev. Chem.*, 2018, **2**, 1–17.
26 J. Mahatthananchai and J. W. Bode, *Acc. Chem. Res.*, 2014, **47**, 696–707.
27 S. M. Mali, S. K. Singh, E. Eid and A. Brik, *J. Am. Chem. Soc.*, 2017, **139**, 4971–4986.
28 J. Liang, L. Zhang, X.-L. Tan, Y.-K. Qi, S. Feng, H. Deng, Y. Yan, J.-S. Zheng, L. Liu and C.-L. Tian, *Angew. Chem., Int. Ed.*, 2017, **56**, 2744–2748.
29 Y. Zhang, T. Hirota, K. Kuwata, S. Oishi, S. G. Gramani and J. W. Bode, *J. Am. Chem. Soc.*, 2019, **141**, 14742–14751.
30 C. J. White and J. W. Bode, *ACS Cent. Sci.*, 2018, **4**, 197–206.
31 G. N. Boross, D. Schauenburg and J. W. Bode, *Helv. Chim. Acta*, 2019, **102**, e1800214, DOI: **10.1002/hlca.201800214**.
32 D. Schauenburg, M. Divandari, K. Neumann, C. A. Spiegel, T. Hackett, Y.-C. Dzeng, N. D. Spencer and J. W. Bode, *Angew. Chem., Int. Ed.*, 2020, **59**, 14656–14663.
33 A. M. Dumas, G. A. Molander and J. W. Bode, *Angew. Chem., Int. Ed.*, 2012, **51**, 5683–5686.
34 H. Noda, G. Erős and J. W. Bode, *J. Am. Chem. Soc.*, 2014, **136**, 5611–5614.
35 D. Mazunin, N. Broguiere, M. Zenobi-Wong and J. W. Bode, *ACS Biomater. Sci. Eng.*, 2015, **1**, 456–462.
36 D. Mazunin and J. W. Bode, *Helv. Chim. Acta*, 2017, **100**, e1600311.
37 A. Fracassi, J. Cao, N. Yoshizawa-Sugata, É. Tóth, C. Archer, O. Gröninger, E. Ricciotti, S. Y. Tang, S. Handschin, J.-P. Bourgeois, A. Ray, K. Liosi, S. Oriana, W. Stark, H. Masai, R. Zhou and Y. Yamakoshi, *Chem. Sci.*, 2020, **11**, 11998–12008.
38 A. L. Rychel, K. M. Peterson and K. U. Torii, *J. Plant Res.*, 2010, **123**, 275–280.
39 L. G. L. Richardson and K. U. Torii, *J. Exp. Bot.*, 2013, **64**, 5243–5251.
40 L. J. Pillitteri and K. U. Torii, *Annu. Rev. Plant Biol.*, 2012, **63**, 591–614.
41 X. Zhang, W. Liu, T. T. Nagae, H. Takeuchi, H. Zhang, Z. Han, T. Higashiyama and J. Chai, *Nat. Commun.*, 2017, **8**, 1331.
42 A. Huber, L. Galgóczy, G. Váradi, J. Holzknecht, A. Kakar, N. Malanovic, R. Leber, J. Koch, M. A. Keller, G. Batta, G. K. Tóth and F. Marx, *Biochim. Biophys. Acta, Biomembr.*, 2020, **1862**, 183246.
43 H. Liu, L. Zhao, J. Zhang, C. Li, X. Shen, X. Liu, W. Jiang, C. Luo, Y. Wang, L. Che and Y. Xu, *Front. Physiol.*, 2019, **10**, 464.
44 A. Hallmann, *Plant Signaling Behav.*, 2008, **3**, 124–127.
45 A. Huber, D. Hajdu, D. Bratschun-Khan, Z. Gáspári, M. Varbanov, S. Philippot, Á. Fizil, A. Czajlik, Z. Kele, C. Sonderegger, L. Galgóczy, A. Bodor, F. Marx and G. Batta, *Sci. Rep.*, 2018, **8**, 1751.
46 B. Fahnert, J. Veijola, G. Roël, M. K. Kärkkäinen, A. Railo, O. Destrée, S. Vainio and P. Neubauer, *J. Biol. Chem.*, 2004, **279**, 47520–47527.
47 X. Liu, H. Zhang, H. Jiao, L. Li, X. Qiao, M. R. Fabrice, J. Wu and S. Zhang, *BMC Genomics*, 2017, **18**, 610.
48 E. Marshall, L. M. Costa and J. Gutierrez-Marcos, *J. Exp. Bot.*, 2011, **62**, 1677–1686.
49 S. Zhong, M. Liu, Z. Wang, Q. Huang, S. Hou, Y.-C. Xu, Z. Ge, Z. Song, J. Huang, X. Qiu, Y. Shi, J. Xiao, P. Liu, Y.-L. Guo, J. Dong, T. Dresselhaus, H. Gu and L.-J. Qu, *Science*, 2019, **364**, eaau9564.
50 H. Takeuchi and T. Higashiyama, *PLoS Biol.*, 2012, **10**, e1001449.
51 N. Uchida, J. S. Lee, R. J. Horst, H.-H. Lai, R. Kajita, T. Kakimoto, M. Tasaka and K. U. Torii, *Proc. Natl. Acad. Sci. U. S. A.*, 2012, **109**, 6337–6342.
52 S. Sprunck, U. Baumann, K. Edwards, P. Langridge and T. Dresselhaus, *Plant J.*, 2005, **41**, 660–672.
53 T. Tameshige, S. Okamoto, J. S. Lee, M. Aida, M. Tasaka, K. U. Torii and N. Uchida, *Curr. Biol.*, 2016, **26**, 2478–2485.
54 A. F. Haag, B. Kerscher, S. Dall'Angelo, M. Sani, R. Longhi, M. Baloban, H. M. Wilson, P. Mergaert, M. Zanda and G. P. Ferguson, *J. Biol. Chem.*, 2012, **287**, 10791–10798.
55 S. Lu and M. C. Edwards, *Phytopathology*, 2016, **106**, 166–176.
56 K. A. T. Silverstein, W. A. Moskal Jr, H. C. Wu, B. A. Underwood, M. A. Graham, C. D. Town and K. A. VandenBosch, *Plant J.*, 2007, **51**, 262–280.
57 D. Wang, L. Tian, D.-D. Zhang, J. Song, S.-S. Song, C.-M. Yin, L. Zhou, Y. Liu, B.-L. Wang, Z.-Q. Kong, S. J. Klosterman, J.-J. Li, J. Wang, T.-G. Li, S. Adamu, K. V. Subbarao, J.-Y. Chen and X.-F. Dai, *Mol. Plant Pathol.*, 2020, **21**, 667–685.
58 K. Hara, R. Kajita, K. U. Torii, D. C. Bergmann and T. Kakimoto, *Genes Dev.*, 2007, **21**, 1720–1725.
59 K. Hara, T. Yokoo, R. Kajita, T. Onishi, S. Yahata, K. M. Peterson, K. U. Torii and T. Kakimoto, *Plant Cell Physiol.*, 2009, **50**, 1019–1031.
60 L. Hunt and J. E. Gray, *Curr. Biol.*, 2009, **19**, 864–869.
61 S. S. Sugano, T. Shimada, Y. Imai, K. Okawa, A. Tamai, M. Mori and I. Hara-Nishimura, *Nature*, 2010, **463**, 241–244.
62 K. U. Torii, *Trends Plant Sci.*, 2012, **17**, 711–719.
63 S. Ohki, M. Takeuchi and M. Mori, *Nat. Commun.*, 2011, **2**, 512.
64 N. Ke and M. Berkmen, *Curr. Protoc. Mol. Biol.*, 2014, **108**, 16.1B.1-21.
65 A. Singh, V. Upadhyay, A. K. Upadhyay, S. M. Singh and A. K. Panda, *Microb. Cell Fact.*, 2015, **14**, 41.
66 J.-S. Zheng, S. Tang, Y.-K. Qi, Z.-P. Wang and L. Liu, *Nat. Protoc.*, 2013, **8**, 2483–2495.
67 V. R. Pattabiraman, A. O. Ogunkoya and J. W. Bode, *Angew. Chem., Int. Ed.*, 2012, **51**, 5114–5118.
68 C. E. Murar, M. Ninomiya, S. Shimura, U. Karakus, O. Boyman and J. W. Bode, *Angew. Chem., Int. Ed.*, 2020, **59**, 8425–8429.

69 J. W. Bode, *Acc. Chem. Res.*, 2017, **50**, 2104–2115.
70 I. Pusterla and J. W. Bode, *Nat. Chem.*, 2015, **7**, 668–672.
71 T. G. Wucherpfennig, V. R. Pattabiraman, F. R. P. Limberg, J. Ruiz-Rodríguez and J. W. Bode, *Angew. Chem., Int. Ed.*, 2014, **53**, 12248–12252.
72 C. He, S. S. Kulkarni, F. Thuaud and J. W. Bode, *Angew. Chem., Int. Ed.*, 2015, **54**, 12996–13001.
73 F. Rohrbacher, A. Zwicky and J. W. Bode, *Chem. Sci.*, 2017, **8**, 4051–4055.
74 G. N. Boross, S. Shimura, M. Besenius, N. Tennagels, K. Rossen, M. Wagner and J. W. Bode, *Chem. Sci.*, 2018, **9**, 8388–8395.
75 N. Kumarswamyreddy, D. N. Reddy, D. Miklos Robkis, N. Kamiya, R. Tsukamoto, M. M. Kanaoka, T. Higashiyama, S. Oishi and J. W. Bode, *RSC Chem. Biol.*, 2022, **3**, 721–727.
76 M. Mutter, A. Chandravarkar, C. Boyat, J. Lopez, S. Dos Santos, B. Mandal, R. Mimna, K. Murat, L. Patiny, L. Saucède and G. Tuchscherer, *Angew. Chem., Int. Ed.*, 2004, **43**, 4172–4178.
77 Y. Sohma, M. Sasaki, Y. Hayashi, T. Kimura and Y. Kiso, *Chem. Commun.*, 2004, 124–125.
78 T. Yoshiya, A. Taniguchi, Y. Sohma, F. Fukao, S. Nakamura, N. Abe, N. Ito, M. Skwarczynski, T. Kimura, Y. Hayashi and Y. Kiso, *Org. Biomol. Chem.*, 2007, **5**, 1720–1730.
79 Y. Sohma, H. Kitamura, H. Kawashima, H. Hojo, M. Yamashita, K. Akaji and Y. Kiso, *Tetrahedron Lett.*, 2011, **52**, 7146–7148.
80 F. Rohrbacher, S. Baldauf, T. G. Wucherpfennig and J. W. Bode, *Synlett*, 2017, 1929–1933.
81 J. S. Lee, T. Kuroha, M. Hnilova, D. Khatayevich, M. M. Kanaoka, J. M. McAbee, M. Sarikaya, C. Tamerler and K. U. Torii, *Genes Dev.*, 2012, **26**, 126–136.
82 G. Lin, L. Zhang, Z. Han, X. Yang, W. Liu, E. Li, J. Chang, Y. Qi, E. D. Shpak and J. Chai, *Genes Dev.*, 2017, **31**, 927–938.
83 V. I. Martynov, A. A. Pakhomov, N. V. Popova, I. E. Deyev and A. G. Petrenko, *Acta Nat.*, 2016, **8**, 33–46.
84 M. R. L. Stone, M. S. Butler, W. Phetsang, M. A. Cooper and M. A. T. Blaskovich, *Trends Biotechnol.*, 2018, **36**, 523–536.
85 N. Kumar, Y. Hori and K. Kikuchi, *J. Biochem.*, 2019, **166**, 121–127.
86 T. Meckel, A. C. Hurst, G. Thiel and U. Homann, *Plant J.*, 2004, **39**, 182–193.
87 J. S. Lee, M. Hnilova, M. Maes, Y.-C. L. Lin, A. Putarjunan, S.-K. Han, J. Avila and K. U. Torii, *Nature*, 2015, **522**, 439–443.
88 X. Qi, A. Yoshinari, P. Bai, M. Maes, S. M. Zeng and K. U. Torii, *eLife*, 2020, **9**, e58097.